

Quality inspection of critical aircraft engine components: towards full automation

Original

Quality inspection of critical aircraft engine components: towards full automation / Cannizzaro, Davide; Simone, Filomena; Illgner-Fehns, Klaus; Mata, Sara; Mondino, Ivan; Ghiazza, Alberto; Poncino, Massimo; Di Cataldo, Santa. - ELETTRONICO. - (2022). (Intervento presentato al convegno 2022 27th IEEE International Conference on Emerging Technologies and Factory Automation (ETFA) tenutosi a Stuttgart (DE) nel 6th-9th September 2022) [10.1109/ETFA52439.2022.9921542].

Availability:

This version is available at: 11583/2971330 since: 2022-09-15T17:31:42Z

Publisher:

IEEE

Published

DOI:10.1109/ETFA52439.2022.9921542

Terms of use:

This article is made available under terms and conditions as specified in the corresponding bibliographic description in the repository

Publisher copyright

IEEE postprint/Author's Accepted Manuscript

©2022 IEEE. Personal use of this material is permitted. Permission from IEEE must be obtained for all other uses, in any current or future media, including reprinting/republishing this material for advertising or promotional purposes, creating new collecting works, for resale or lists, or reuse of any copyrighted component of this work in other works.

(Article begins on next page)

Quality inspection of critical aircraft engine components: towards full automation

1st Davide Cannizzaro
Politecnico di Torino

Torino, Italy
davide.cannizzaro@polito.it

2nd Filomena Simone
K|Lens GmbH

Saarbrücken, Germany
filomena.simone@k-lens.de

3rd Klaus Illgner-Fehns
K|Lens GmbH

Saarbrücken, Germany
klaus.illgner-fehns@k-lens.de

4th Sara Mata
IDEKO

Elgoibar, Spain
smata@ideko.es

5th Ivan Mondino

Avio Aero, GE Aviation
Rivalta di Torino, Italy
ivan.mondino@avioaero.it

6th Alberto Ghiazza

Avio Aero, GE Aviation
Rivalta di Torino, Italy
alberto.ghiazza@avioaero.it

7th Massimo Poncino

Politecnico di Torino
Torino, Italy
massimo.poncino@polito.it

8th Santa Di Cataldo

Politecnico di Torino
Torino, Italy
santa.dicataldo@polito.it

Abstract—The quality of products has become a key factor for success in the current manufacturing industry. This is especially true in the aviation field where components for aircraft engines called honeycombs are produced. Due to their small dimension and peculiar shape, such components typically undergo a severe and cumbersome visual inspection by specialized operators. However, this process is highly prone to human error, requires a lot of time and a high number of undetected defects have been reported. In order to reduce the whole inspection time, ensure higher quality and guarantee standardization and process control, this paper presents an innovative strategy for the fully-automated inspection of honeycomb engine parts. The proposed solution is a two-phase process fully controlled by a robot, leveraging a camera as well as a purposely designed optic fibers sensor, coupled with Artificial Intelligence (AI) algorithms for the detection of different types of defects. To assess the functionality and validity of the proposed solution, a fully functioning prototype is described and characterized.

Index Terms—Artificial Intelligence, Complex automation system, Computer Vision, Industry 4.0, Robotics

I. INTRODUCTION

Nowadays, with the development of industry 4.0 plants, companies are moving towards the automation of production lines, but in most cases the visual inspection of the final product is still carried out manually by a human operator. However, the manual inspection of the parts could lead to misjudgment due to subjective analysis, human tendencies, environment, and characteristics of the part [1], [2]. The visual inspection may vary depending on the part produced [3]. For example, in the aerospace field, the production of honeycomb parts for the engines is one of the most demanding in terms of accuracy, complexity, and time required [4]. A honeycomb part is typically composed of several hexagonal cells connected to each other with different height and slope (see Fig. 1). During production, the honeycomb cells are bound to a metal support through a hot metal fluid [5]. The produced part is exposed to strong thermal phenomena, leading to different types of external or internal defects that compromise the performance of the honeycomb [6] (see Fig. 1).

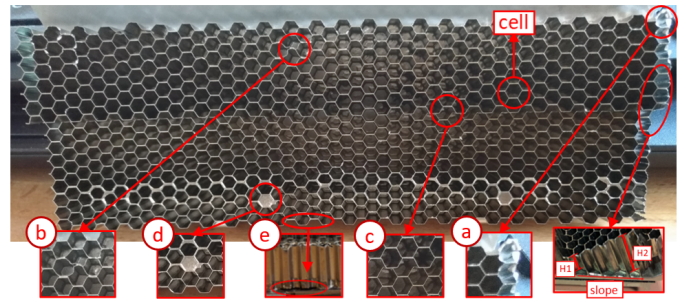


Fig. 1. Honeycomb structure and defects: a) missing cells, b) damaged cells, c) opened cells, d) excessive bond material and e) not bonded cells.

In order to ensure the quality of the finished part, the structure is thoroughly examined by an operator [7], putting in place specific visual inspection procedures tailored for the different categories of defects: i) *external defects* are inspected by visually observing the part and measuring the size and type of faults as well as the number of missing or damaged cells; ii) *internal defects* are inspected by manually passing an inspection light through each cell of the honeycomb, looking for any light dispersion due to incorrect bonding of the structure (*light-bleeding* approach). The manual inspection can address the damages that are either in the honeycomb wall basements (internal) or in the honeycomb wall medium part (external), which are the ones that are most critical and frequent. However, the successful detection of the defects is highly influenced by the ability and experience of the human operator [8]. To overcome the problems of manual inspection, several studies focus on improving the performances of the human operator through training programs or augmented reality [9], [10]. While these works show very promising results, they are still in the early stages and not fully integrated in a real industrial environment [11]. In [12], the authors address the inspection issues of aviation components with non destructive testing. However, these methods require high costly equipment and specialized workers. Starting from these

considerations, the objective of this paper is to propose a completely new approach to fully automatize the inspection of the honeycomb parts, possibly making it more objective and less prone to human errors. In the following sections we describe a real case study developed within the context of the EIT Manufacturing project AVISPA-2, which was fully implemented and characterized in an aviation industry.

II. CASE STUDY ANALYSIS AND DESIGN CONCEPT

In the first stages of our project, we analyzed a limited set of significant samples provided by an aviation company to characterize the most typical defects affecting the parts (see Fig. 1). Based on the characteristics of such defects and on their acceptability requirements, we conceived and designed the automation of the inspection procedure. The observed defects can be divided into two main broad categories:

(i) *External defects*: this category includes defects that can be visually assessed by frontally observing the part, as shown in (Fig. 1 from *a* to *c*). The external defects are all represented by discontinuities in the cell profile patterns detectable by an Artificial Intelligence (AI) framework.

(ii) *Internal defects*: this type of defects (Fig. 1 *c* and *e*) involves the internal structures of the cells. Hence, to solve this problem, we exploit an automatic light-bleeding approach through a glass fiber sensor developed for the case study. To fully automatize the inspection, we integrate robotics, machine vision, artificial intelligence, and smart sensors. The process is conceived as a sequence of two consecutive phases:

Phase 1: In the first phase, a robotic arm moves the camera to take a frontal high-resolution image view of the honeycomb. The camera software takes the image and computes a *disparity map* to provide depth information. The AI framework analyzes the two images and detects external defects and cell coordinates. In case several defects are detected, the inspection ends and the part is rejected. Otherwise, Phase 2 starts.

Phase 2: The second phase detects internal defects. More specifically, the same robotic arm inserts a special glass fiber sensor inside the cells of the honeycomb, scanning the whole part. The light-bleeding method allows to highlight the presence of open cells or not bonded areas. Starting from this concept, we developed a fully functioning demonstrator in a real industrial environment, which is described in details in the following.

III. AUTOMATED INSPECTION SYSTEM

A demonstration robotic set-up was developed in a real industrial plant (see Fig. 2), with the following components.

- 1) *Kuka KR16-2 robot with KRC4 robot controller*: the camera and the glass fiber sensor are attached to the robot flange.
- 2) *Ingesys IC3 controller*: This PLC is used to activate the camera and the glass fiber sensor and to start the acquisition during the inspection procedures.
- 3) *SVS-Vistek hr455CXGE camera and K|Lens 3D lens* (K|Lens technology): A high resolution camera with a proprietary 3D lens is used in the Phase 1 to acquire images.

4) *Optical fiber sensor (K|Lens technology)*: the sensor developed for Phase 2 is composed of several glass fibers and a microcontroller for data processing.

5) *Disparity Map software (K|Lens technology)*: the disparity map software provides depth information about each cell in the honeycomb that are used in Phase 1 for the defect detection.

6) *Artificial Intelligence framework*: the framework is in charge of detecting external defects in Phase 1 by means of automated segmentation techniques.

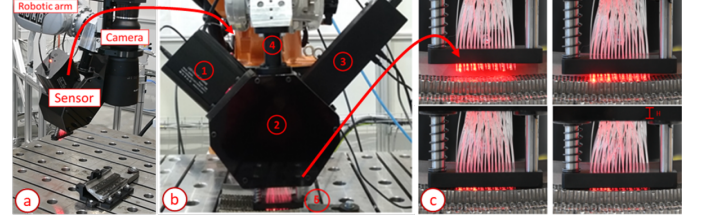


Fig. 2. Inspection set-up: a) Robotic arm with high resolution camera and b) optical fiber sensor prototype with c) glass fiber sliding system developed.

A special tool holder was developed to attach both the glass fiber sensor and the camera to the same robot. The whole integrated system will be hereafter referred to as *the tool*.

A. Robotic and camera set-up

The robot is in charge of moving the tool during the inspection process following an offline programmed trajectory executed by the KRC4 and Ingesys IC3 controllers. The software camera is in charge of taking the images and computing the disparity map for Phase 1. However, each honeycomb part has a complex structure composed of several hexagon shaped cells. Due to the small size of cells, standard stereo systems with large baseline are unfeasible. To overcome these issues, a novel multi-view technology, the K|Lens®, having a very short baseline, is used. This allows to analyze the structure and depth of each cell with better performances and accuracy. A full frame industrial camera (SVS Vistech) is used that is able to acquire images with a resolution of 61Mpx (see Fig. 3-a).

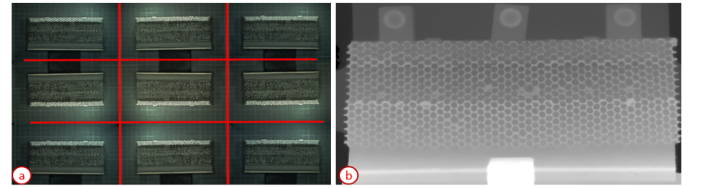


Fig. 3. a) Multi-view image of an honeycomb and b) Disparity map.

B. Disparity Map software

The acquisition of images using a multi-view stereo system allows to extract 3D information. By comparing information about a scene from two different points, the relative depth information can be obtained in the form of a disparity map [13]. As described before, the K|Lens enables with one physical lens to capture 9 perspectives, as shown in Fig. 3-a. In

this Figure, each sub-image looks slightly different from the others, allowing to obtain a disparity map that is more robust than the one derived from two perspectives. In Fig. 3-b an example of disparity map is shown. The depth of each cell is shown using a color scale, where lighter color indicates lower distance to the viewer.

C. Optical fiber sensor

In order to automatize the inspection of internal defects for Phase 2, an optical fiber sensor was developed for this purpose. If a cell is internally damaged, by illuminating it, rays of light are reflected in its neighboring cells. Therefore, by monitoring the neighboring cells, it is possible to understand whether a cell is healthy or damaged. The optical fiber sensor (see Fig. 2-b) is composed of the following parts: i) a powerful LED light generator; ii) two types of glass fibers, the emitting ones (actuators) and the passive ones (sensors); iii) a closed box with a mini camera and a microcontroller; iv) a sensor holder, which enables the connection with the robot end-effector; v) the fiber driving adapter, in which the fibers are collected and driven. In Fig. 2-c, the holder and its fibers at work are shown. The holder has been rigidly connected through screws to metal cylinders. Those ones, instead, are connected to the sensor body through ball bearings, which enable the cylinders to slide when the spring is pressed. The bearings also avoid the transmission of undesired forces to the holder. When the robot end effector moves upward, the spring is released and therefore, the holder regains its original position.

D. Artificial Intelligence framework

The AI framework is in charge of detecting external defects in Phase 1. It is composed of the following modules: i) the *segmentation* module takes the acquired honeycomb image and disparity map as the input and provides a segmentation of the single cell profiles/areas and the coordinates of their centers; ii) the *defect detection* module takes as input a set of quantitative features extracted from the segmentation results and identifies the faulty regions accordingly. In order to detect the main characteristics of the honeycomb and improve the results obtained, the segmentation module is based on a combination of classic approaches (standard edge detectors, adaptive thresholding techniques) and a deep learning architecture specialized for semantic segmentation (U-Net, [14]). To address the issue of low availability of training samples, the defect detection module is developed as an anomaly detection system leveraging a set of ad-hoc rules for each category of defect. The model is trained on small annotated Regions of Interest (ROIs) of the honeycomb image, together with a binary mask of each cell wall. Both the approaches are built on top of standard Python libraries and frameworks for Computer Vision and Deep Learning (OpenCV, Keras, etc.).

IV. EXPERIMENTAL INSPECTION PROCESS

To demonstrate the functionality of the automated process, we performed a full demonstration (Phase 1 + Phase 2) on a few test samples in a real industrial plant. In the following, we describe the obtained results.

A. 1st Phase Inspection

In the first phase, the robot starts from the initial position and moves the fixture with the camera above the honeycomb. When the robot is in position, the camera is triggered and a new multi-view image (kaleidoscopic image) of the part is acquired (Fig. 3). The nine views captured with the camera are pre-processed, cut into individual sub-images, rectified and used to compute the disparity map of the honeycomb as described in the previous section. After the calculation of the disparity map, the two images are collected and provided to the AI framework that analyzes them through a segmentation module that provides a segmentation of the single cell profiles/areas as outcome (Fig. 4, right side) and a defect detection module that takes as input quantitative features extracted from the segmentation results. The defects detection module identifies the faulty regions accordingly, detects the shape of each healthy cell in green and shows the defected cells based on the gravity of cell distortion (red $\geq 30\%$, yellow $< 30\%$ and purple $< 5\%$) (Fig. 4, left side).

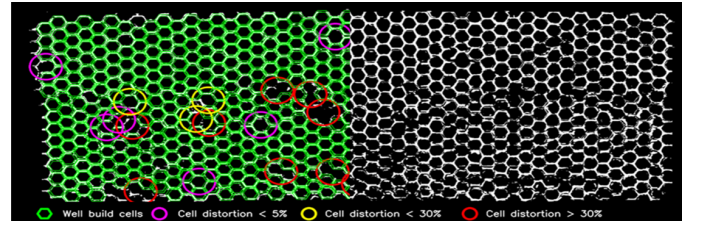


Fig. 4. Example of honeycomb cells segmentation (on the right) and honeycomb defects analysis (on the left).

The analysis allows to detect superficial defects like damaged cells, missing cells, and opened cells together with the coordinates of the center of each cell. The first phase inspection requires $\sim 15s$ on a basic CPU or $\sim 8s$ on a basic GPU, which is well below the time required for a manual inspection.

B. 1st Phase validation

To train and test the AI framework, images of defected honeycombs were taken and a mask of the part was created manually to serve as the ground truth for the honeycomb segmentation. The dataset was built by taking images of 8 different honeycombs, split into two completely independent groups: i) Training honeycombs: the group is composed of 6 honeycombs that are used for training the algorithm and optimizing the parameters. ii) Testing honeycombs: the group is composed of the remaining 2 honeycombs that are used solely for testing purposes. The training/testing images were acquired with two different experimental settings: i) Off-process: this setting was implemented in a laboratory with the camera mounted in a fixed position above the part. Of the 95 off-process images that were acquired, 75 were included in the training group and 20 in the testing one. ii) In-process: this is the setting of the integrated demonstrator built in a real industrial environment. Due to logistics difficulties, it includes only 20 images taken and added to the testing group.

Finally, we performed two different testing experiments. The first experiment (*off-process testing*) trains the model with the training group (composed only of off-process images) and tests it with the off-process testing ones. The second experiment (*in-process testing*) trains the model with the off-process training images and tests it with the in-process testing ones. This experimental configuration allows to further verify the robustness of the model to environmental conditions that are sensibly different from the ones used for training. The results of such two experiments are the following: i) Off-process: accuracy: 87.99%, sensitivity: 70.31%, specificity: 88.37%; ii) In-process: accuracy: 76.89%, sensitivity: 60.68%, specificity: 77.36%. As it was reasonable to expect, the off-process testing metrics showed better results. However, the in-process testing experiment shows a reduction of accuracy that is reasonably limited (around 11%), and above 60% for all the metrics. One can conclude that the model performance is reasonably good in the given challenging experimental conditions, with a large room for future improvements.

C. 2nd Phase Inspection

After the inspection of the honeycomb in Phase 1, if no critical external defects are detected, Phase 2 is carried on. In this case, the robot places the optical fiber sensor inside the cells and 24 glass fibers are lighted in order to inspect the neighbors cells (see Fig 2-c). At the same time, the remaining fibers are monitored by the mini camera located inside the body of the tool to sense unexpected light. An image is acquired by the mini camera and processed by the microcontroller, if no light is detected from the sensing fibers, the microcontroller returns that the analyzed cells are healthy (Fig. 5, left side) otherwise return that the cells are damaged (Fig. 5, right side).



Fig. 5. Interface with the microcontroller output: a) Healthy part, blue dots represent healthy cells. b) Damaged part, red dots represent damaged cells.

With this procedure, the whole inspection of the honeycomb for Phase 2 can be carried on. All the experiments for Phase 2 were directly carried out on the real plant showing up promising results in detecting internal defects with a 100% accuracy.

V. CONCLUSIONS AND FUTURE WORK

This paper proposes a new approach to automatize the inspection procedure of complex honeycomb parts in the aviation industry. The proposed 2-phases inspection process results to be fast and robust. The objective criteria for inspection provided by the aviation field allows our automatic procedure to be particularly effective in replacing the human role. The automatic inspection is able to identify with a good level of

accuracy and robustness all different types of defects (either internal or external) that may be the cause of rejection of the part, using a two phases procedure. The performance of Phase 1 can be largely improved in the future by enlarging the training set with many more honeycombs parts and defect examples. For Phase 2, a first prototype of honeycomb sensor is designed and manufactured, which is able to successfully detect internal damages of the cells. In the future, sensor shape and weight will be largely improved. At the present stage, the total estimated inspection time is in the range of 40-60s, which is a very promising result. Future works will focus on improving the acquisition and image pre-processing stage, as well as on optimizing the processing stages in order to reduce the inspection time by at least a half. Unlike manual inspection, the procedure is completely repeatable, and the obtained results are traceable and documentable in every part.

ACKNOWLEDGMENT

This work was pursued within the project AVISPA-2 funded by EIT Manufacturing with code 21054.



REFERENCES

- [1] A. Kujawińska *et al.*, "The role of human motivation in quality inspection of production processes," in *Advances in Ergonomics of Manufacturing: Managing the Enterprise of the Future*. Springer, 2016, pp. 569–579.
- [2] K. A. Latorella *et al.*, "A review of human error in aviation maintenance and inspection," *Human Error in Aviation*, pp. 521–549, 2017.
- [3] A. Hobbs, "An overview of human factors in aviation maintenance," *ATSB Safety Report, Aviation Research and Analysis Report AR*, vol. 55, p. 2008, 2008.
- [4] R. T. Kidangan *et al.*, "Detection of dis-bond between honeycomb and composite facesheet of an inner fixed structure bond panel of a jet engine nacelle using infrared thermographic techniques," *Quantitative InfraRed Thermography Journal*, pp. 1–15, 2020.
- [5] J. Wittenauer *et al.*, "Structural honeycomb materials for advanced aerospace designs," *JOM*, vol. 42, no. 3, pp. 36–41, 1990.
- [6] Z. Wang *et al.*, "On the influence of structural defects for honeycomb structure," *Composites Part B: Engineering*, vol. 142, pp. 183–192, 2018.
- [7] C. G. Drury *et al.*, "Good practices in visual inspection," *Human factors in aviation maintenance-phase nine, progress report, FAA/Human Factors in Aviation Maintenance*, 2002.
- [8] C. Franciosi *et al.*, "A taxonomy of performance shaping factors for human reliability analysis in industrial maintenance," *Journal of Industrial Engineering and Management*, vol. 12, no. 1, pp. 115–132, 2019.
- [9] R. J. Jacob *et al.*, "Improving inspector's performance and reducing errors-general aviation inspection training systems (gaits)," in *Proceedings of the Human Factors and Ergonomics Society Annual Meeting*, vol. 48, no. 1. SAGE Publications Sage CA: Los Angeles, CA, 2004, pp. 203–207.
- [10] K. S. Aggour *et al.*, "Artificial intelligence/machine learning in manufacturing and inspection: A ge perspective," *MRS Bulletin*, vol. 44, no. 7, pp. 545–558, 2019.
- [11] X. Fang *et al.*, "Research progress of automated visual surface defect detection for industrial metal planar materials," *Sensors*, vol. 20, no. 18, p. 5136, 2020.
- [12] K. David, "Nondestructive inspection of composite structures: methods and practice," in *17th world conference on nondestructive testing, Shanghai*. Citeseer, 2008.
- [13] R. A. Hamzah *et al.*, "Literature survey on stereo vision disparity map algorithms," *Journal of Sensors*, vol. 2016, 2016.
- [14] O. Ronneberger *et al.*, "U-net: Convolutional networks for biomedical image segmentation," in *International Conference on Medical image computing and computer-assisted intervention*. Springer, 2015, pp. 234–241.